Novel features of a fully developed mixing-layer between co-flowing laminar and turbulent Couette flows

Vagesh D. Narasimhamurthy, Helge I. Andersson, and Bjørnar Pettersen

Citation: Physics of Fluids (1994-present) **26**, 031703 (2014); doi: 10.1063/1.4868645
View online: http://dx.doi.org/10.1063/1.4868645
View Table of Contents: http://scitation.aip.org/content/aip/journal/pof2/26/3?ver=pdfcov
Published by the AIP Publishing

PHYSICS OF FLUIDS **26**, 031703 (2014)

Novel features of a fully developed mixing-layer between co-flowing laminar and turbulent Couette flows

Vagesh D. Narasimhamurthy,[1,a)] Helge I. Andersson,[1] and Bjørnar Pettersen[2]
[1]*Department of Energy and Process Engineering, Norwegian University of Science and Technology (NTNU), NO-7491 Trondheim, Norway*
[2]*Department of Marine Technology, NTNU, NO-7491 Trondheim, Norway*

(Received 27 November 2013; accepted 3 March 2014; published online 20 March 2014)

A new flow configuration has been proposed in which a bilateral mixing-layer exists in the junction between co-flowing laminar and turbulent plane Couette flows. Contrary to a classical plane mixing-layer, the present mixing-layer did neither grow in time nor in streamwise direction. However, the mixing zone varied with the distance from the stationary wall. A direct numerical simulation showed that very-large-scale flow structures were found in the turbulent part of the flow with Reynolds number 1300 based on half the velocity U_1 of the fastest-moving wall and half of the distance $2h$ between the walls. The laminar-turbulent interface exhibited a large-scale meandering motion with frequency $0.014U_1/h$ and wavelength about $25h$. Large-scale Taylor-Görtler-like roll cells were observed in the nominally laminar flow region with Reynolds number 260. This tailor-made flow is particularly well suited for explorations of momentum transfer and intermittency in the vicinity of the laminar-turbulent interface.
 [http://dx.doi.org/10.1063/1.4868645]

When two fluid streams of different velocities or of different densities interact, a mixing zone is established which is popularly called *mixing-layer* in fluid mechanics.[1–3] Depending on the Reynolds number, plane mixing-layers can be turbulent, which finds importance not only in atmospheric and oceanic flows but also in many industrial applications, such as turbo-machinery, internal combustion engines, gas lasers, heat-exchangers, etc. A salient feature of turbulent plane mixing-layers is that they belong to the category of *free-shear flows*, where the mixing- or shear-zone is in between two fluid streams and is free from any wall interactions. In addition, plane mixing-layers are known to grow either in the streamwise direction or in time. By contrast, we define a new problem in the current work, where we aim to investigate the mixing-zone at the junction of two co-flowing plane Couette flows. Figure 1(a) defines the current problem, where two plane Couette flows are placed in a side-by-side arrangement. The junction between the two Couette flows lies midway along the y-direction, i.e., at $y = 8.4h$ (where h is the channel half-height). The arrangement consists of a stationary wall at the bottom ($z = 0$) and two co-moving walls at the top ($z = 2h$), where the individual wall velocities are U_1 and U_2 (such that $U_1 > U_2$). This implies that the two parts of the top wall that are moving in the x-direction are not only in relative motion with each other but also in relative motion to the stationary bottom wall. Thereby, the fluid that fills the gap between the walls, from $z = 0$ to $z = 2h$, is subjected to a complex three-dimensional shearing motion. The current problem is unique since a mixing-layer is established in a wall-bounded shear-flow environment rather than as a classical free shear flow. In addition, the present flow configuration has a potential to shed light on the dynamics of the turbulent/non-turbulent interfaces,[4,5] which has triggered recent interest in the research community.[6–9] One way of realizing the current problem in a laboratory is by means of a Taylor-Couette flow apparatus, where the driving cylinder may be split into two parts

a)Email: vagesh@alumni.ntnu.no

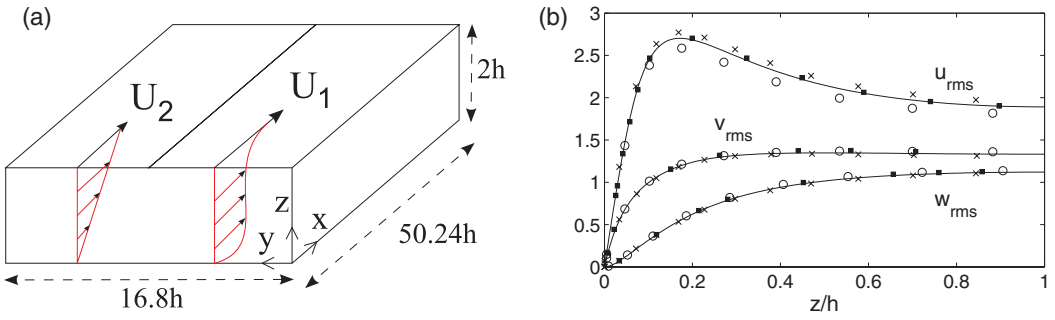

FIG. 1. (a) The computational domain used for two co-flowing plane Couette flows with wall velocities U_1 and $U_2 < U_1$. (b) Variation of root-mean-square values of fluctuating velocities normalized by wall-friction velocity u_τ in a single turbulent plane Couette flow ($Re = Uh/2\nu = 1300$): −, present; ○, Bech *et al.*;[16] ■, Hu *et al.*;[18] ×, Holstad *et al.*[19]

with each part rotating at a different speed.[10] Note that the Taylor-Couette flow, where the fluid is confined in the gap between two rotating concentric cylinders, approaches the plane Couette flow in the limit of large radii and small gaps.[11] In practise, the current problem of two co-flowing Couette flows mimics the flow interaction beneath two adjacent trains or two adjacent ships in side-by-side operation. Note that the flow beneath a flat-bottomed ship (very large crude carrier) that travels with a small underkeel clearance to a flat sea bed represents plane Couette flow.[12]

In the present case, we define Reynolds numbers based on half the velocity difference between the moving and the stationary wall and the channel half-height h, i.e., the higher Reynolds number $Re_1 = U_1 h/2\nu$ and the lower Reynolds number $Re_2 = U_2 h/2\nu$. Note that the subcritical transition Reynolds number Re_c for plane Couette flow is in between 300 and 370 and the Reynolds number for establishing fully developed turbulence is 500–600 (see literature reviews in Refs. 13 and 14).

In the present study, we choose direct numerical simulation (DNS) as the computational tool. DNS gives complete access to the instantaneous three-dimensional velocity and pressure fields. The full Navier-Stokes equations for an incompressible and isothermal flow are solved using the parallel finite-volume code MGLET.[15] The code uses staggered Cartesian grid arrangements. Spatial discretization of the convective and diffusive fluxes is carried out using a second-order central-differencing scheme. The momentum equations are advanced in time by a fractional time-stepping using a second-order explicit Adams-Bashforth scheme. The Poisson equation for the pressure is solved by a full multi-grid method based on pointwise velocity-pressure iterations. The computational grid is divided into an arbitrary number of sub-grids that are treated as dependent grid blocks and computed in parallel. As shown in Figure 1(a), the size of the computational domain in each coordinate direction $L_x \times L_y \times L_z$ is $50.24h \times 16.8h \times 2h$, i.e., significantly larger than that in the turbulent plane Couette flow DNS of Bech *et al.*[16] In addition, Holstad *et al.*[17] using two-point correlation data from their turbulent plane Couette flow DNS concluded that the present domain size is appropriate for the Reynolds number considered. A very fine mesh of $640 \times 320 \times 192$ grid points is used in the current DNS. Uniform grid spacing is adopted in the streamwise and the spanwise directions with a grid resolution (in viscous units) of $[\Delta_x^+, \Delta_y^+] = [6.64, 4.44]$, respectively. A non-uniform mesh is used in the wall-normal direction, where the grid resolution close to the walls is set to $\Delta_z^+ = 0.2$ and at the channel mid-plane $\Delta_z^+ = 2.3$. A grid verification simulation performed for a single turbulent plane Couette flow at $Re = 1300$ showed excellent agreement with literature data (see Figure 1(b)). In addition, a coarser grid simulation of the present case of co-flowing laminar and turbulent Couette flows was performed for further verification.[20] The current non-dimensional time-step $\Delta t = 0.002$ is sufficiently small compared to the normalized Kolmogorov time-scale $\tau_\eta U_1/h = hU_1/\nu Re_1^{3/2} = 0.055$. As in most DNSs of plane turbulent Couette flow,[16–19,23] periodic boundary conditions are used in the streamwise and spanwise directions. The plane Couette flow exhibits much longer flow structures than the corresponding Poiseuille flow and therefore a domain length about five times longer than for Poiseuille flow simulations (i.e., about $60h$) is required; see, e.g., Holstad *et al.*[19] Here, $L_x \approx 50h$ is only marginally shorter than the recommended domain length and suffices to decorrelate the flow field between inflow and outflow boundaries.

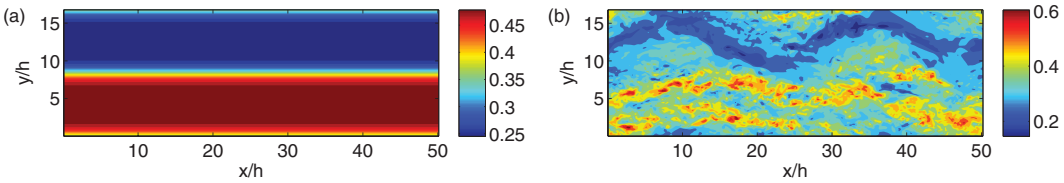

FIG. 2. Instantaneous streamwise velocity u/U_1 in the channel midplane ($z = h$). (a) Two co-flowing laminar Couette flows (where $Re_1 = 260$ and $Re_2 = 130$)[21] and (b) two co-flowing laminar-turbulent Couette flows (where $Re_1 = 1300$ and $Re_2 = 260$).

In Narasimhamurthy *et al.*,[21] the wall-velocity ratio was set to $U_1/U_2 = 2$ and both Re_1 and Re_2 were lower than Re_c, i.e., 260 and 130, respectively. Thereby, the entire flow was in the laminar regime. The numerical solution in Narasimhamurthy *et al.*[21] converged to a steady state. A snapshot of the resulting velocity field is shown in Figure 2(a). It can be observed that the flow field essentially consists of two laminar Couette flows with a steady shear-layer in between. Contrary to the classical free-shear layer,[1] the shear-layer width exhibited a wall-normal variation but was found to be independent of the streamwise position. An analytic solution was also derived for this steady shear-layer and an explicit formula was found for the shear-layer width as a function of the wall-normal distance.

In the current study, the Reynolds numbers are significantly increased so that the right half of the domain in Figure 1(a) is in a supercritical (turbulent) state, while the left half of the domain is initially in a subcritical (laminar) state. The chosen Re and velocity ratio are $Re_1 = 1300$ and $Re_2 = 260$ and $U_1/U_2 = 5$, respectively. Figure 2(b) shows striking features of the computed flow field. It is readily seen in Figure 2 that the stability of the interfacial shear-layer observed at lower Reynolds numbers[21] in Figure 2(a) does no longer prevail at higher Re in Figure 2(b) where the instantaneous isocontours of the streamwise velocity exhibit a winding pattern. Despite this somewhat unexpected behavior, the mixing-layer between the low-speed and high-speed flows does not grow in the streamwise direction. The width of the mixing zone is accordingly independent of x. This particular feature contrasts with the typical mixing-layer[1,2] which widens with downstream distance. The snapshot in Figure 2(b) also suggests that the interface between the non-turbulent and turbulent parts of the flow is winding, contrary to the case in Figure 2(a). Moreover, the turbulent half of the flow (i.e., $y/h < 8.4$) consists of very-large-scale flow structures as typically found in turbulent plane Couette flow experiments[22] and simulations,[16,23] see, for example, Figure 3(a). The instantaneous λ_2-contours in Figure 3(b), conditioned on either positive or negative ω_x or ω_z, show that the turbulent vortices are concentrated in two winding bands. The cross-sectional plot of the mean velocity vectors in Figure 3(c) furthermore shows that the fluid motion perpendicular to the main flow primarily consists of large-scale counter-rotating roll cells. Such roll cells look like Taylor-Görtler cells which may arise in a rotating plane Couette flow due to an instability caused by the presence of the Coriolis force; see, e.g., Bech and Andersson.[25] This instability is present in both the laminar and the turbulent flow regimes. Here, the Taylor-Görtler-like (TGL) roll cells are also present in the low-speed and nominally laminar half of the flow. We conjecture that the very-large-scale structures found in a turbulent plane Couette flow trigger the onset of the winding flow pattern and also tend to convect vortical flow structures from the turbulent to the laminar flow region. The motions associated with the TGL roll cells are relatively weak as compared with the primary x-directed flow. The magnitude of the mean secondary-motion shown in Figure 3(c) is about 1.5% of U_1, whereas the instantaneous secondary-motion is of the order of 20%.

Upon closer examination of Figures 2(b) and 3(b), it may seem that the wavelength of this periodic-wave is about $25h$. This is more conclusive in Figure 4, where iso-surfaces of the instantaneous enstrophy $\omega_i\omega_i$ are shown near the moving walls in Figure 4(a) and in the channel midplane in Figure 4(b). The streamwise wavelength of the meandering flow field has to be equal to the streamwise domain length divided by an integer N, i.e., L_x/N. This is a consequence of the periodicity imposed in the streamwise direction. A visual inspection of the snapshots of the flow field in Figures 2(b), 3(b), and 4(b) readily shows that $N = 2$. The streamwise wavelength is therefore

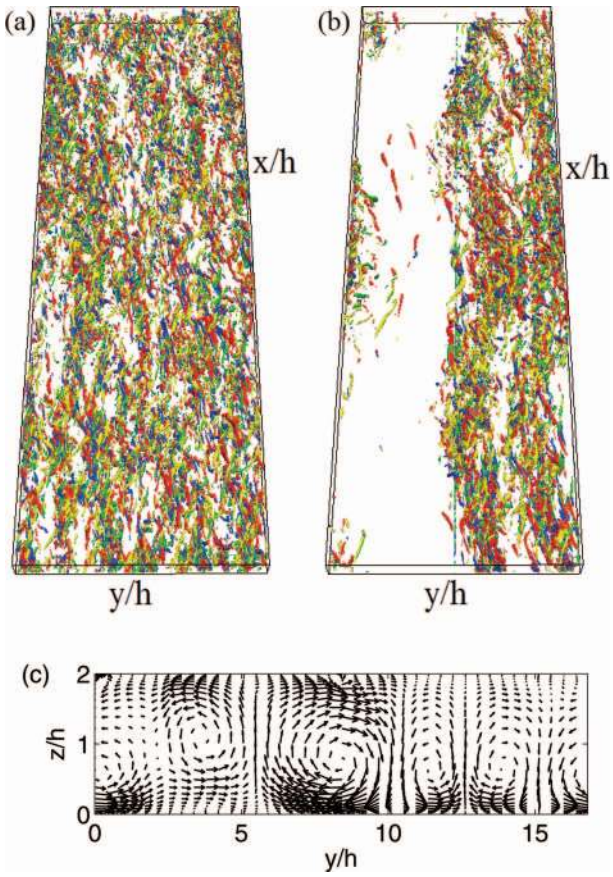

FIG. 3. Instantaneous three-dimensional vortical structures: (a) turbulent plane Couette flow ($Re = 1300$); (b) present co-current laminar and turbulent Couette flows. Contours indicate iso-surfaces of positive and negative components of $\lambda_2\omega_x$ and $\lambda_2\omega_z$, where ω_i is vorticity and λ_2 is defined as in Jeong and Hussain[24] to identify the vortex cores. (c) Appearance of Taylor-Görtler-like (TGL) roll cells in the current mixing-layer. The fully turbulent part of the flow is to the left ($y < 8.4h$).

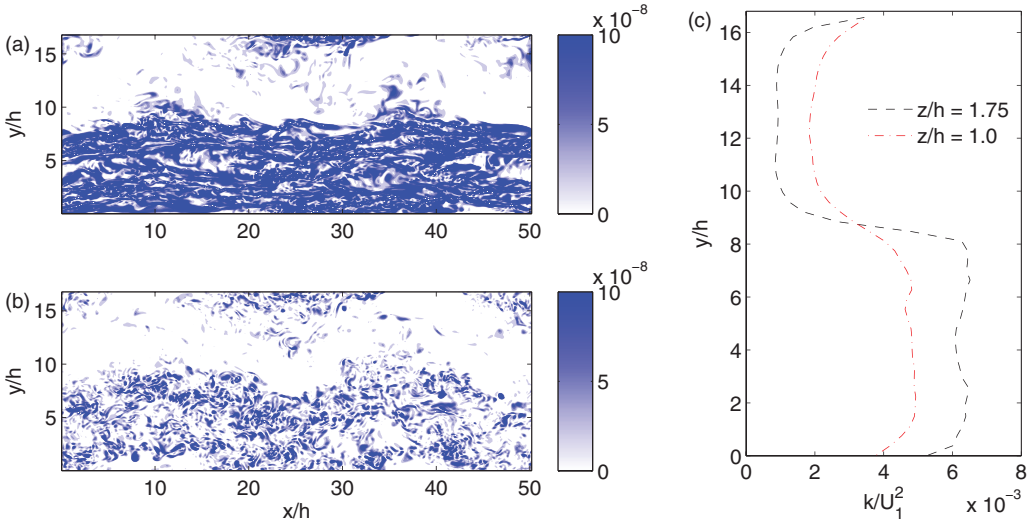

FIG. 4. Instantaneous enstrophy $\omega_i\omega_i\ \nu^2/U_1^4$ at (a) $z/h = 1.75$ and (b) $z/h = 1.0$. (c) Mean turbulent kinetic energy profiles.

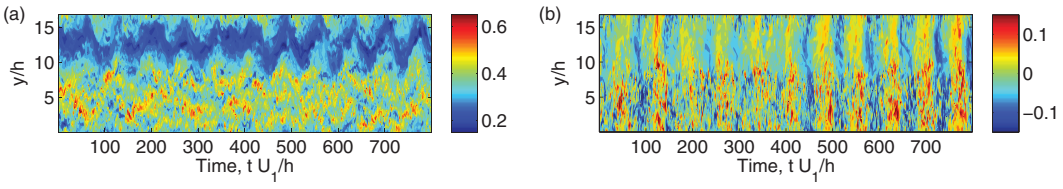

FIG. 5. Time traces of the (a) streamwise velocity u/U_1 and (b) spanwise velocity v/U_1. Sampling line along the span is located at channel midplane ($z = h$).

$50.24h/2.0 \approx 25h$. The numerical value 25 obviously depends on the choice of the domain length L_x and 25 should only be considered as a rough estimate. If, for instance, $N = 1$ then the wavelength would be $\approx 50h$ and if $N = 3$ then the wavelength would be $50.24h/3.0 \approx 17h$. We can therefore conclude from our observations that the wavelength is larger than $17h$ but smaller than $50h$. It should be recalled that the computational domain used in this study is about four times longer than routinely used in channel flow simulations. Although the wavelength of the observed undulations inevitably depends on L_x further extensions were not considered.

In order to provide a quantitative measure of the width of the transition zone between the turbulent and non-turbulent flow, the spanwise variation of the mean turbulent kinetic energy k is shown in Figure 4(c). A distinct drop in k is seen to occur around $y = 8.4h$ and the width of the transition zone is about $1h$ $0.25h$ from the moving walls and circa $3h$ midway between the walls. The k-profiles in Figure 4(c) are broadened by averaging both in time and streamwise direction, similarly as the averaged interface of a turbulent jet in an otherwise quiescent fluid. The modest k-level which remains at the non-turbulent side results from disturbances from the fully turbulent part of the flow.

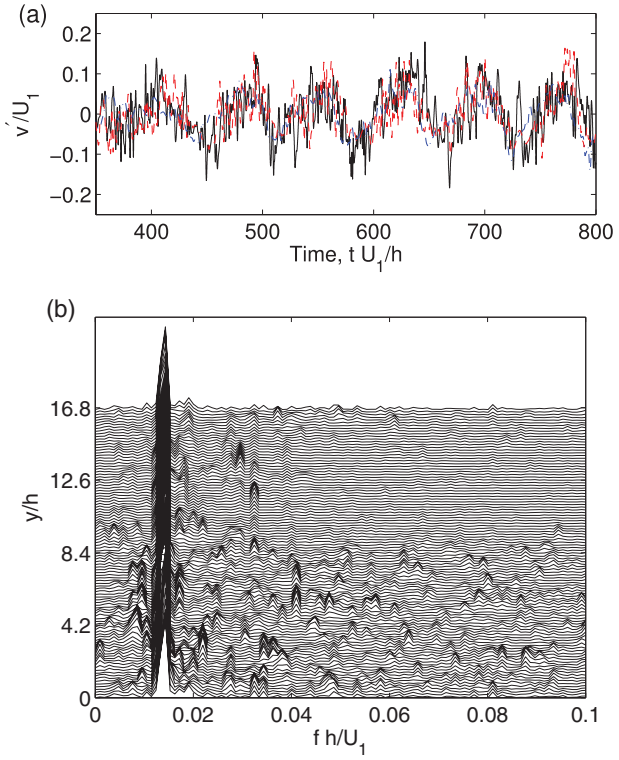

FIG. 6. (a) Time traces of the spanwise velocity fluctuation v'/U_1. Sampling points are located at channel midplane at various spanwise positions: −, $y/h = 4.2$; −−, $y/h = 8.4$; −. −, $y/h = 12.6$. (b) Spectral frequencies fh/U_1 obtained from Fourier analysis of the spanwise velocity fluctuations v'/U_1 sampled at channel midplane. The primary frequency of the meandering motion corresponds to $fh/U_1 = 0.014$.

In order to quantify the time-period of the meandering motion, instantaneous velocities are sampled along a line located at the channel midplane ($z = h$) and oriented in the y-direction. Figure 5 indicates that the present mixing-layer is fully developed and it is not evolving in time but rather oscillates in a periodic fashion. The time traces in Figure 6(a) further elucidate this inference. The sampled data are fed to a fast Fourier transform (FFT) algorithm to obtain the Fourier spectra. Figure 6(b) shows the spectral frequencies. The primary frequency f of the meandering motion corresponds to a Strouhal number $fh/U_1 = 0.014$. The characteristic time scale of the interfacial undulations is therefore about $70h/U_1$ and thus substantially longer than any other time scale in the flow field.

For the first time a new flow configuration has been considered in this letter. This computational set-up enables in-depth investigations of the momentum transfer at the interface between fully developed laminar and turbulent plane Couette flows. Although the mixing-layer between the two co-current streams neither evolves in space nor in time, the mixing zone inevitably varies with the distance from the fixed wall. Somewhat surprising, however, the interface between the turbulent and the non-turbulent flow exhibited substantial large-scale undulations with a wavelength of about $25h$. These slow modulations of the otherwise steady-state mean motions were characterized by a time scale $70h/U_1$. It is particularly noteworthy that the meandering of the two co-current streams persisted across the entire span and tended to destabilize the flow even in the subcritical Couette flow. It is conjectured that this phenomenon is due to an instability of the bilateral, i.e., three-dimensional, mixing-layer which did not occur at the lower Reynolds numbers recently considered by Narasimhamurthy *et al.*[21]

The authors express their gratitude to The Research Council of Norway for financial support through the KMB project "Investigating Hydrodynamic Aspects and Control Strategies for Ship-to-Ship Operations" (RCN 179522/I40) at MARINTEK and also for a grant of computing time (Programme for Supercomputing).

[1] R. C. Lock, "The velocity distribution in the laminar boundary layer between parallel streams," Quart. J. Mech. Appl. Math. **IV**, 42–63 (1951).
[2] G. L. Brown and A. Roshko, "On density effects and large structure in turbulent mixing layers," J. Fluid Mech. **64**, 775–816 (1974).
[3] C.-M. Ho and P. Huerre, "Perturbed free shear layers," Annu. Rev. Fluid Mech. **16**, 365–424 (1984).
[4] S. Corrsin and A. L. Kistler, "Free-stream boundaries of turbulent flows," NACA Technical Report No. TN-1244, Washington, DC, 1955.
[5] D. K. Bisset, J. C. R. Hunt, and M. M. Rogers, "The turbulent/non-turbulent interface bounding a far wake," J. Fluid Mech. **451**, 383–410 (2002).
[6] C. B. da Silva and R. J. N. dos Reis, "The role of coherent vortices near the turbulent/non-turbulent interface in a planar jet," Philos. Trans. R. Soc. A **369**, 738–753 (2011).
[7] C. M. de Silva, J. Philip, K. Chauhan, C. Meneveau, and I. Marusic, "Multiscale geometry and scaling of the turbulent-nonturbulent interface in high Reynolds number boundary layers," Phys. Rev. Lett. **111**, 044501 (2013).
[8] Y. Duguet, O. Le Maître, and P. Schlatter, "Stochastic and deterministic motion of a laminar-turbulent front in a spanwisely extended Couette flow," Phys. Rev. E **84**, 066315 (2011).
[9] C. B. da Silva, J. C. R. Hunt, I. Eames, and J. Westerweel, "Interfacial layers between regions of different turbulence intensity," Annu. Rev. Fluid Mech. **46**, 567–590 (2014).
[10] S. Å. Ellingsen and H. I. Andersson, "Mixing layer between two co-current Taylor-Couette flows," Eur. J. Mech. B **37**, 23–28 (2013).
[11] H. Faisst and B. Eckhardt, "Transition from the Couette-Taylor system to the plane Couette system," Phys. Rev. E **61**, 7227–7230 (2000).
[12] T. Gourlay, "Flow beneath a ship at small underkeel clearance," J. Ship Res. **50**, 250–258 (2006).
[13] T. M. Schneider, F. D. Lillo, J. Buehrle, B. Eckhardt, T. Dörnemann, K. Dörnemann, and B. Freisleben, "Transient turbulence in plane Couette flow," Phys. Rev. E **81**, 015301 (2010).
[14] L. S. Tuckerman and D. Barkley, "Patterns and dynamics in transitional plane Couette flow," Phys. Fluids **23**, 041301 (2011).
[15] M. Manhart, "A zonal grid algorithm for DNS of turbulent boundary layers," Comput. Fluids **33**, 435–461 (2004).
[16] K. H. Bech, N. Tillmark, P. H. Alfredsson, and H. I. Andersson, "An investigation of turbulent plane Couette flow at low Reynolds numbers," J. Fluid Mech. **286**, 291–325 (1995).
[17] A. Holstad, P. S. Johansson, H. I. Andersson, and B. Pettersen, "On the influence of domain size on POD modes in turbulent plane Couette flow," in *Proceedings of the 6th Direct and Large-Eddy Simulation (DLES6), Poitiers, September 2005*, edited by E. Lamballais *et al.* (ERCOFTAC Series, 2006), Vol. 10, pp. 763–770.
[18] Z. Hu, C. L. Morfey, and N. D. Sandham, "Sound radiation in turbulent channel flows," J. Fluid Mech. **475**, 269–302 (2003).

[19] A. Holstad, H. I. Andersson, and B. Pettersen, "Turbulence in a three-dimensional wall-bounded shear flow," Int. J. Numer. Meth. Fluids **62**, 875–905 (2010).
[20] V. D. Narasimhamurthy, H. I. Andersson, and B. Pettersen, "Aspects of a turbulent-nonturbulent interface," J. Phys.: Conf. Ser. **318**, 022017 (2011).
[21] V. D. Narasimhamurthy, S. Å. Ellingsen, and H. I. Andersson, "Bilateral shear layer between two parallel Couette flows," Phys. Rev. E **85**, 036302 (2012).
[22] O. Kitoh, K. Nakabyashi, and F. Nishimura, "Experimental study on mean velocity and turbulence characteristics of plane Couette flow: Low-Reynolds-number effects and large longitudinal vortical structure," J. Fluid Mech. **539**, 199–227 (2005).
[23] T. Tsukahara, H. Kawamura, and K. Shingai, "DNS of turbulent Couette flow with emphasis on the large-scale structure in the core region," J. Turbul. **7**, N19 (2006).
[24] J. Jeong and F. Hussain, "On the identification of a vortex," J. Fluid Mech. **285**, 69–94 (1995).
[25] K. H. Bech and H. I. Andersson, "Secondary flow in weakly rotating turbulent plane Couette flow," J. Fluid Mech. **317**, 195–214 (1996).